Pergamon

Int. J. Solids Structures Vol. 35, No. 7–8, pp. 665–685, 1998

0020–7683/98 $19.00 + .00

PII: S0020–7683(97)00081–4

ANALYTICAL PROBABILISTIC MODELING OF INITIAL FAILURE AND RELIABILITY OF LAMINATED COMPOSITE STRUCTURES

SERGEI P. YUSHANOV†
University of Akron, Department of Polymer Engineering, Akron, Ohio 44325-0301, U.S.A.

and

ALEXANDER E. BOGDANOVICH†

North Carolina State University, Department of Textile Engineering, Chemistry and Science, Raleigh, North Carolina 27695-8301, U.S.A.

(*Received* 24 *June* 1996; *in revised form* 26 *February* 1997)

Abstract—An analytical approach based on the theory of stochastic processes is developed for the stochastic initial failure analysis and reliability predictions of thin-walled laminated composite structures. The probability of initial failure is calculated using theory of rare passages of the random strain vector field out of the prescribed region of allowable states. The region is limited by the ultimate strain surfaces adopted for each individual layer in the laminate. The surfaces, in their turn, are defined in terms of the scatters in the ultimate strains for the composite layer. Reliability function of a composite layer having random elastic characteristics and loaded with random in-plane tractions is determined through the probability of its initial failure. The reliability function of the laminated composite structure is then calculated through the failure probabilities of individual layers, using the weakest link model. The proposed approach allows one to solve diverse stochastic problems and requires substantially less computational expenses than Monte Carlo simulation technique. The approach may be invaluable for a quick evaluation of various competitive design projects when considering laminated composite structures under the reliability constraint. Applications of the developed approach are illustrated on the examples of reliability predictions of laminated composite cylindrical shells under the effect of random internal pressure and laminated composite plates under random biaxial loading. Numerical results reveal specific probabilistic phenomena related to the effects of ply lay-up, scatters in mechanical and strength characteristics and random loading histories. Results obtained from the developed analytical approach are compared to those calculated with Monte Carlo simulation technique. © 1997 Elsevier Science Ltd

1. INTRODUCTION

Deformation and failure processes in composite structural parts occurring during their in-service failure are, essentially, of a stochastic nature. The processes depend on a number of random factors:

- manufacturing imperfections, for example scatters of stiffness and strength characteristics of a composite lamina, imperfect bonding between the layers, various geometrical irregularities;
- uncertainties introduced through the assembly processes, for example variability of the interaction conditions between the parts in bolted, adhesive and other types of joints;
- inevitably random nature of the in-service mechanical loads and environmental conditions.

An attempt to realistically address the aforementioned as well as other possible stochastic effects in the analysis and design of real-life composite structures would lead to an extremely complex probabilistic/stochastic problem. There are several known options to approach the problem. One of them, which is currently dominating, is Monte Carlo simulation technique. This approach is theoretically simple, does not require substantial analytical work, is able to address diverse stochastic problems. On the other side, this

† Current address: AdTech Systems Research, Inc., Beavercreek, Ohio 45432-2698, U.S.A.

usually requires a huge amount of computer time and memory, especially when finite element methods or other numerical techniques are used for stress calculations. Indeed, when considering highly reliable structures, it is necessary to run hundreds (possibly, even thousands) computational variants ("realizations") in order to predict a single numerical value—reliability of the structure under specified loading conditions.

Another option is to develop analytical probabilistic models. Following this approach, one would be able to establish explicit relations between the random input data and the output reliability value. This approach is theoretically more complex, requires application of the advanced concepts of the theory of probability, stochastic processes and reliability. However, in return, this provides powerful tools for the quick reliability evaluation considering many possible loading conditions, material properties and other design parameters. It should be emphasized that both aforementioned approaches, while very distinct, can be combined together, depending on the specific needs of the designer.

Generally, the goal of a stochastic structural analysis can be formulated as the "behavior" prediction of the structure which is exposed to some random in-service conditions and possesses intrinsic stochastic properties itself. The behavior can be formalized in terms of the region of allowable states which is defined in a multi-dimensional space of displacements strains/stresses. Thus, only those values of these characteristics that belong to the interior of the region, are permitted during lifetime of the structure. Any violation of this condition is commonly treated as partial "refusal" of the structure, Bolotin (1982). Mathematically, this problem can be formulated in terms of the reliability function which is defined as probability of the event that the structure works without any refusals. Consequently, any refusal lowers the reliability value. The condition identifying the occurrence of any single refusal can be formulated using various criteria. The maximum allowable point-wise deflection is a reasonable one in the problems of buckling, see Bogdanovich and Yushanov (1981). Probabilistic analogues of the maximum stress/maximum strain criteria represent more complex point-wise ultimate condition, see Bogdanovich and Yushanov (1983), Yushanov (1985). Depending on the criterion, each refusal can be viewed as the cause of partial or total exhaustion of the load-carrying capacity of the structure.

The theory characterizing progressive "damage build-up" in composite materials has been developed by Bolotin (1976), (1981). Each damage occurrence is treated as partial refusal which is random event. From this point, progressive damage in composite material or structure can be characterized as stochastic vector process. In the specific case of laminated composite structures it is natural, following the philosophy of deterministic mechanics of laminated structures, to assume that each layer, viewed as the basic structural entity, may experience its own set of refusals. If the very first refusal occurring in some layer is treated as the end of service life of the structure, then the stochastic analogue of the deterministic first-ply failure analysis is obtained. If numerous "partial" refusals are permitted up to the point when some "ultimate" refusal occurs, then the stochastic analogue of the deterministic ply-by-ply failure analysis is obtained. The examples of "initial" stochastic failure analysis of laminated composite cylindrical shells can be found in Protasov *et al.* (1978), where Monte Carlo modeling has been used, in Bogdanovich and Yushanov (1983), (1986), (1994), Yushanov (1985a), where analytical modeling using theory of stochastic processes has been developed. Various approaches for "progressive", ply-by-ply stochastic failure analysis were presented in Protasov *et al.* (1980), (1983) using the Monte Carlo method and in Yushanov (1985b), Bogdanovich and Yushanov (1987) using theory of stochastic vector processes. Another original analytical approach for progressive failure analysis of laminated composite plates, based on the idea of gradual reduction of stiffness distribution functions of the layer, has been developed in Dzenis *et al.* (1992), (1993), (1994). This utilizes theory of stochastic vector processes as well.

Among a few other works devoted to probabilistic/stochastic analysis of laminated composite plates and shells the following ones should be mentioned. The reliability of laminated composite plates subjected to in-plane loads has been studied in Cassenti (1984), Nakagiri *et al.* (1987), Tani *et al.* (1988), Cederbaum *et al.* (1990), Thomas and Wetherhold (1991), Corvi and Vangi (1992). Specifically, the failure criterion of Hashin has been used as the "performance function" in Cederbaum *et al.* (1990). Due to the reason that this

performance function is nonlinear with respect to the ply stresses, the Hasofer-Lind method was used for its linearization in the vicinity of the design point. The distance from the stress space origin to the ultimate surface is then treated as the reliability index.

Probabilistic geometrically nonlinear finite element analyses were recently developed by Engelstad and Reddy (1992) for thin-walled composite shells and by Kam *et al.* (1993) for thin-walled composite plates. In the former work, the first-order second-moment approach was used to calculate random fields. A reliability analysis has been performed using the Tsai-Wu first ply failure criterion. In the latter work, random strength properties and random loads were accounted for. The ultimate surfaces were obtained by performing a series of first ply failure analyses following different paths in the multiaxial load space. The maximum work, maximum strain and maximum stress-first-ply failure criteria were utilized. The first of them is nonlinear, so the Hasofer-Lind linearization method has been applied, similarly to the earlier work of Cederbaum *et al.* (1990).

A structural synthesis problem has been discussed in Thanedar and Chamis (1995) in the context of integrating the reliability-based strength requirements and optimization techniques for the tailoring process of composite structures. As pointed out in this work, "almost all of the existing structural tailoring software is based on a deterministic approach. Thus, it is not possible to directly account for the inherent composite properties scatter in the currently available tailoring software." This conclusion emphasizes the necessity of developing advanced probabilistic approaches which would address all random factors essential for laminated composite structures and provide theoretical background for economical and diverse design software.

The objective of this work is to develop a general approach for the reliability analysis of thin laminated composite plates and shells, using theory of stochastic vector processes. The approach can be viewed as a probabilistic extension of classical theory of laminated plates and shells and its application for the first ply failure prediction based on the probabilistic analogue of the maximum strain/stress criteria. The analysis takes into account scatters in elastic and strength ply properties along with the random quasistatic loading history.

2. PROBABILISTIC MESOVOLUME ANALYSIS

Any composite can be treated as a multi-element system consisting of some "fundamental entities". Depending on the specific needs of the analysis, a single fiber element surrounded by a matrix material (a "microvolume") or a monolayer consisting of a great amount of microvolumes (a "mesovolume") or a larger part of the whole structure (a "macrovolume") can be considered as the fundamental entity. The principal assumption adopted here is that the mesovolume should contain a sufficiently large number of microvolumes and can, therefore, be viewed as a structurally homogeneous body. In each specific case, the mesovolume has to be chosen as to satisfy the following requirements:

(i) "structural" homogeneity of the material at the mesovolume level, and

(ii) "stochastic" homogeneity of displacements, strains, and stresses inside the mesovolume.

In the simplest case, when all of the layers in the laminated structure are under uniform strains and stresses, each of them can be treated as a single mesovolume. In the case of nonuniform strain/stress fields inside the structure, the size of the mesovolume has to be determined by the characteristic scale of the variation of stress and strain fields. It has to be pointed out that the conditions (i) and (ii) may be controversial, and it is easy to imagine situations where, under sharply varying stress-strain states, no entity satisfying both the conditions (i) and (ii) can be found.

Assuming that decomposition of the structure into a number of mesovolumes has been established, the reliability function can be defined as follows. Considering some mesovolume, the "performance" vector $\mathbf{q}(\mathbf{r}, t)$ that characterizes different "states" of the mesovolume during the loading history is introduced. The components of this vector can be, specifically, the components of the displacement vector, stress or strain tensors. Thus,

the performance vector characterizes stochastically homogeneous random field created in the mesovolume during the loading history. Further, the region of allowable states Ω should be defined in the respective displacement/strain/stress space. Like in the deterministic mechanics, this is performed by prescribing some "ultimate surface" Γ which is mathematically defined in terms of the selected phenomenological point-wise failure criterion. The only difference with the traditional failure analysis is that the surface Γ is now of a stochastic nature. This means that the ultimate displacements, strains or stresses are random values. For example, in the case of stochastic maximum stress criterion, the region Ω is a multi-dimensional parallelepiped with the boundary Γ defined by several random values. In the case of tensor-polynomial criteria, the corresponding regions Ω are ellipsoids defined by respective random values, etc.

Thus, for an arbitrary mesovolume, the first task is to calculate probability of the event that the performance vector escapes from the region of allowable states Ω. If the calculations show that such an event had occurred, a partial or total refusal of the mesovolume is stated, and this should be accounted in the further stochastic deformation and failure processes. The mesovolume reliability function, R_s, is then determined as probability that no one refusal had occurred in this mesovolume during the time interval under consideration. Theory of passages of random functions or processes out of the region of allowable states can be used for calculating this probability, Bolotin (1982).

After the reliability function of each individual mesovolume has been determined, it remains to define reliability of the multi-element system (in our case, the assemblage of N mesovolumes), using their individual reliability functions $R_1, R_2, \ldots, R_N$. In the simplest approach, assuming that failures of the mesovolumes are stochastically independent events, the following two utmost reliability values can be obtained. First, considering that laminated structure is an assemblage of the mesovolumes linked in series, the reliability function is determined by the formula

$$R' = \prod_{s=1}^{N} R_s. \tag{1}$$

In the case of parallel connection, it is defined as

$$R'' = 1 - \prod_{s=1}^{N} (1 - R_s). \tag{2}$$

The reliability value intermediate between (1) and (2) can be obtained using some parameters that characterize accumulation of the "partial refusals" (various definitions of the "defectiveness levels" or "damageability parameters" were used in Bolotin (1976), Protasov *et al.* (1980), Yushanov (1985b), Bogdanovich and Yushanov (1987)). The damageability parameter can be introduced, for example, as $\omega = n/N$, where n is the number of refused mesovolumes. In general, the reliability of each remaining mesovolume is influenced by all of the previous refusals in the same mesovolume or in other mesovolumes which belong to the same structure. To take account of the whole "refusal history", it is necessary to establish a specific model of stochastic stiffness reductions, respective stress redistributions, etc. In other words, it is necessary to develop a complex stochastic model of progressive damage in a multi-element structure. Various approaches to this problem have been proposed in Protasov *et al.* (1980), Yushanov (1985b), Bogdanovich and Yushanov (1987), Dzenis *et al.* (1992), (1993), (1994). However, in this initial study our objective is not to dwell into this very complex problem, but to calculate reliability of each individual mesovolume in the laminated structure and then obtain reliability of the multi-element structure using the series connection model (1).

Thus, the state of the sth mesovolume is characterized by the performance vector $\mathbf{q}^{(s)}(t) = \{q_1^{(s)}(t), \ldots, q_k^{(s)}(t)\}$ which is a random function of time but is independent of the spatial coordinates. Let the region of allowable states be specified as follows:

$$\Omega: q_i^- \leqslant q_i^{(s)} \leqslant q_i^+, \quad i = 1, \ldots, k. \tag{3}$$

If the performance vector is specified in the strain space, then its components are the components of the strain tensor $\hat{\varepsilon}^{(s)}(t)$. If the performance vector is specified in the stress space, then its components are the components of the stress tensor $\hat{\sigma}^{(s)}(t)$. The region of allowable states Ω is limited by the ultimate surface Γ which is specified in the space of ultimate strains or stresses by a set of parameters $q_i^{\pm}$, which are random values with the mean values $\langle q_i^{\pm} \rangle$ and the standard deviations $\sigma_{q_i^{\pm}}$. Parameters $\sigma_{q_i^{\pm}}$ are determined by the scatter of ultimate stresses/strains of the material.

Each passage of the performance vector $\mathbf{q}^{(s)}(t)$ out of the region Ω is a refusal of the layer. The probability of the event that the vector $\mathbf{q}^{(s)}(t)$ does not leave the region Ω within the preset time interval $0 \leqslant \tau \leqslant t$ defines the reliability of the mesovolume:

$$R_s(t) = \Pr\{\mathbf{q}^{(s)}(\tau) \in \Omega; \quad 0 \leqslant \tau \leqslant t\}. \tag{4}$$

In the following, the composite structures under consideration are assumed to be systems with high reliability index and, accordingly, the probability (4) is expressed in terms of the expected rate, $\nu[\mathbf{q}^{(s)}(t)]$, of the crossings of the ultimate surface by the vector $\mathbf{q}^{(s)}(t)$ per unit time:

$$R_s(t) = \exp\left\{-\int_0^t \nu[\mathbf{q}^{(s)}(\tau)]\, \mathrm{d}\tau\right\}. \tag{5}$$

For highly reliable systems, the expected rate of crossings, $\nu[\mathbf{q}^{(s)}(t)]$, can be calculated as the sum of the expected rates of the crossings per unit time by each component of the performance vector:

$$\nu[\mathbf{q}^{(s)}(t)] = \sum_{i=1}^{k} \{\nu[q_i^{(s)}(t); q^-] + \nu[q_i^{(s)}(t); q^+]\}. \tag{6}$$

In eqn (6), $\nu(q_i^{(s)}, q^+)$ is the expected rate of the q^+ level-up-crossing for component $q_i^{(s)}$ and $\nu(q_i^{(s)}; q^-)$ is the expected rate of the q^- level-down-crossing for component $q_i^{(s)}$. The rates are expressed in terms of the differential distribution, $f(q_i^{(s)}, \dot{q}_i^{(s)})$, of the ordinates of respective random function and its derivative, Sveshnikov (1968):

$$\nu(q_i^{(s)}; q^-) = \int_{-\infty}^{0} f(q^-, \dot{q}_i^{(s)}) |\dot{q}_i^{(s)}|\, \mathrm{d}\dot{q}_i^{(s)}; \quad \nu(q_i^{(s)}; q^+) = \int_0^{\infty} f(q^+, \dot{q}_i^{(s)}) \dot{q}_i^{(s)}\, \mathrm{d}\dot{q}_i^{(s)}. \tag{7}$$

If the performance vector is Gaussian process, then $f(q_i^{(s)}, \dot{q}_i^{(s)})$ is the two-dimensional normal distribution, and integration in eqn (7) can be carried out to obtain a close form solution (Bolotin, 1982). If the centered performance vector is a stationary random process, then the two-dimensional normal distribution reduces to the product of the one-dimensional distributions, $f(q_i^{(s)}, \dot{q}_i^{(s)}) = f_1(q_i^{(s)}) f_2(\dot{q}_i^{(s)})$, and eqn (7) after performing the integration yields

$$\nu[q_i(t); q^{\pm}] = \frac{1}{2\pi} \frac{\sigma_{\dot{q}_i}(t)}{\sqrt{\sigma_{q_i}^2(t) + \sigma_{q_i^{\pm}}^2}} \exp\left[-\frac{(\langle q_i(t) \rangle - \langle q_i^{\pm} \rangle)^2}{2(\sigma_{q_i}^2(t) + \sigma_{q_i^{\pm}}^2)}\right] \times \left\{\exp\left[\frac{\langle \dot{q}_i(t) \rangle}{2\sigma_{\dot{q}_i}^2(t)}\right] \pm \sqrt{2\pi}\Phi\left(\pm \frac{\langle \dot{q}_i(t) \rangle}{\sigma_{\dot{q}_i}(t)}\right)\right\} \tag{8}$$

where

$$\Phi(u) = \frac{1}{2\pi}\int_{-\infty}^{u} \exp\left(-\frac{x^2}{2}\right)\mathrm{d}x$$

is the Laplace function. For the brevity of the notations, the superscript (s) of the performance vector is dropped here and henceforth. The following notations are further introduced in (8): $\sigma_{q_i}^2(t) = K_{q_iq_i}(t,t)$ and

$$\sigma_{\dot{q}_i}^2(t) = \left.\frac{\partial^2 K_{q_iq_i}(t_1,t_2)}{\partial t_1 \partial t_2}\right|_{t_1=t_2=t}$$

are the variances of the random function $q_i(t)$ and its derivative, respectively; $\sigma_{q_i^{\pm}}^2 = \langle (q_i^{\pm} - \langle q_i^{\pm}\rangle)^2\rangle$ is the variance of the ultimate parameters; $K_{q_iq_j}(t_1,t_2)$ is the (i,j)th element of the second rank covariance tensor $\hat{\mathbf{K}}_{\mathbf{q}}(t_1,t_2)$:

$$\hat{\mathbf{K}}_{\mathbf{q}}(t_1,t_2) = \langle \mathring{\mathbf{q}}(t_1) \otimes \mathring{\mathbf{q}}(t_2)\rangle$$

$$= \begin{bmatrix} \langle \mathring{q}_1(t_1)\mathring{q}_1(t_2)\rangle & \cdots & \langle \mathring{q}_1(t_1)\mathring{q}_j(t_2)\rangle & \cdots & \langle \mathring{q}_1(t_1)\mathring{q}_k(t_2)\rangle \\ & & \cdots & \cdots & \cdots \\ & & \langle \mathring{q}_i(t_1)\mathring{q}_j(t_2)\rangle & \cdots & \langle \mathring{q}_i(t_1)\mathring{q}_k(t_2)\rangle \\ & & & \cdots & \cdots \\ & \text{sym} & & & \langle \mathring{q}_k(t_1)\mathring{q}_k(t_2)\rangle \end{bmatrix}. \tag{9}$$

Here, symbol $\langle \ldots \rangle$ stands for mathematical expectation, symbol $\otimes$ stands for outer tensor multiplication, and the top symbol "$\circ$" denotes the centered random variable: $\mathring{x} = x - \langle x\rangle$.

In eqn (8), the group of terms in the curly brackets accounts for the possible time variation of the mean value of the performance vector. If $\langle \dot{q}_i(t)\rangle = 0$, then the sum of the terms in curly brackets is equal to unity, and eqn (8) reduces to the rate of a random level crossing by a stationary process. The inner "static" stochastic properties of the system (such as scatter in material elastic properties) are taken into account by the term σ_{q_i}, while the "nonstationary" stochastic properties (as in the case of dynamic random loading) are accounted for by the term $\sigma_{\dot{q}_i}$. Ultimate stochastic properties (specifically, the scatter in strength characteristics) are accounted for by the terms $\sigma_{q^{\pm}}$.

Thus, in order to calculate a mesovolume reliability function, it is necessary to calculate first the covariance tensors of the performance vector and its derivatives.

3. STIFFNESS COVARIANCE ANALYSIS

When using classical theory of multidirectional laminates, the constitutive relations are of the form

$$\begin{bmatrix} \mathbf{N} \\ \mathbf{M} \end{bmatrix} = \begin{bmatrix} \hat{\mathbf{A}} & \hat{\mathbf{B}} \\ \hat{\mathbf{B}} & \hat{\mathbf{D}} \end{bmatrix} \begin{bmatrix} \mathbf{e} \\ \mathbf{k} \end{bmatrix} \tag{10}$$

where $\mathbf{N}$ and $\mathbf{M}$ are the vectors of stress resultants and moments, $\mathbf{e}$ and $\mathbf{k}$ are the vectors of the strain components on the reference plane (mid-plane) and curvature of the laminate, $\hat{\mathbf{A}}$ is the matrix of extensional stiffnesses, $\hat{\mathbf{B}}$ is the matrix of coupling stiffnesses, and $\hat{\mathbf{D}}$ is the matrix of bending or flexural laminate stiffnesses. The laminate stiffness matrices $\hat{\mathbf{A}}$, $\hat{\mathbf{B}}$, and $\hat{\mathbf{D}}$ are expressed in terms of the stiffness matrices of the individual layers, $\hat{\mathbf{Q}}'^{(s)}$, through the common equations, Jones (1975). Further, under the assumption of a plane stress state, $\hat{\mathbf{Q}}'^{(s)}$ are expressed in terms of the reduced stiffness matrix, $\hat{\mathbf{Q}}$, and the ply lay-up angles φ_s by applying rotation through angle φ_s about the normal to the laminate mid-plane. Finally,

elements of $\hat{\mathbf{Q}}$ are expressed, for each individual layer, in terms of the engineering constants of the composite material.

Due to assumed scatter in elastic properties of the layer, elements of $\hat{\mathbf{Q}}$ are random values. Consequently, all elements of the laminate stiffness matrices, $\hat{\mathbf{A}}$, $\hat{\mathbf{B}}$, and $\hat{\mathbf{D}}$, are random values. Hence, the constitutive relations (10) are stochastic equations. Furthermore, the performance vector $\mathbf{q}^{(s)}(t)$ depends on the laminate stiffnesses. Thus, in order to calculate the covariance tensor (9) of the performance vector, the covariance tensors of the laminate stiffnesses must be first obtained. Our current aim is to express the covariance tensors of the laminate stiffnesses in terms of prescribed mean values and standard deviations of the lamina engineering constants.

Let us introduce random vector $\mathbf{X}$ whose components are the minimum set of independent engineering constants of a lamina. Also, introduce the following random stiffness vectors: $\mathbf{Q}$, $\mathbf{Q}'$, $\mathbf{A}$, $\mathbf{B}$, and $\mathbf{D}$. Components of these vectors are rearranged non-zero distinct elements of the stiffness matrices $\hat{\mathbf{Q}}$, $\hat{\mathbf{Q}}'$, $\hat{\mathbf{A}}$, $\hat{\mathbf{B}}$, and $\hat{\mathbf{D}}$, respectively. For example, in the case of an orthotropic lamina there are, considering a plane stress case, four independent engineering constants; accordingly, $\mathbf{X} = \{E_{11}^{(s)}, E_{22}^{(s)}, G_{12}^{(s)}, \nu_{12}^{(s)}\}$. Thus, the vector of membrane stiffnesses of the laminate is $\mathbf{A} = \{A_{11}, A_{12}, A_{16}, A_{22}, A_{26}, A_{66}\}$.

The reduced stiffnesses depend on the ply elastic constants in a rather complex, nonlinear manner. Hence, calculation of the stiffness covariances cannot be performed directly. To overcome this difficulty, we will apply the linearization procedure to the functions of random variables. In the procedure, the vector of reduced stiffnesses is expanded into the power series in the vicinity of the mean values of its arguments:

$$\mathring{\mathbf{Q}} = \mathbf{Q} - \langle \mathbf{Q} \rangle = \left. \frac{\partial \mathbf{Q}}{\partial \mathbf{X}} \right|_{\mathbf{X} = \langle \mathbf{X} \rangle} \cdot (\mathbf{X} - \langle \mathbf{X} \rangle) + \cdots \approx (\mathbf{Q} \nabla_X)|_{\mathbf{X} = \langle \mathbf{X} \rangle} \cdot \mathring{\mathbf{X}} \tag{11}$$

where higher-than-linear terms have been neglected. Here, symbol "·" stands for scalar product (inner tensor product), and $\mathbf{Q}\nabla_X$ is the second rank tensor with its (i,j)th component equal to $\partial Q_i / \partial X_j$. Using (11) and definition of the covariance function and the identity $(\mathbf{Q}\nabla_X) \cdot \mathring{\mathbf{X}} \equiv \mathring{\mathbf{X}} \cdot \nabla_X \mathbf{Q}$, one obtains the following covariance tensor of the reduced ply stiffnesses:

$$\langle \mathring{\mathbf{Q}} \otimes \mathring{\mathbf{Q}} \rangle = \mathbf{Q} \nabla_X |_{\mathbf{X} = \langle \mathbf{X} \rangle} \cdot \langle \mathring{\mathbf{X}} \otimes \mathring{\mathbf{X}} \rangle \cdot (\nabla_X \mathbf{Q})|_{\mathbf{X} = \langle \mathbf{X} \rangle} \tag{12}$$

where $\nabla_X \mathbf{Q}$ is second rank tensor with its (i,j)th component being equal to $\partial Q_j / \partial X_i$. Since the ply elastic constants are independent, all components of the second rank tensor $\langle \mathring{\mathbf{X}} \otimes \mathring{\mathbf{X}} \rangle$ are zero except those which belong to the main diagonal. The diagonal components are equal to the corresponding variances of the ply elastic constants. Equation (12) is then written in the following form

$$\langle \mathring{Q}_i \mathring{Q}_j \rangle = \sum_l \sigma_{X_l}^2 \left. \frac{\partial Q_i}{\partial X_l} \frac{\partial Q_j}{\partial X_l} \right|_{\mathbf{X} = \langle \mathbf{X} \rangle} \tag{13}$$

where $\sigma_{X_l}^2 = \langle \mathring{X}_l^2 \rangle$ is the variance of the engineering constant X_l. Vector $\mathbf{Q}'^{(s)}$ is expressed in terms of the vector $\mathbf{Q}$ and the ply lay-up angle φ_s:

$$\mathbf{Q}'^{(s)} = \hat{\mathbf{b}}^{(s)} \cdot \mathbf{Q} \tag{14}$$

where $\hat{\mathbf{b}}^{(s)}$ is the standard transformation matrix for rotation through angle φ_s about the normal to the laminate mid-surface. With the use of (14), the covariance tensor of reduced ply stiffnesses (related to the "global" coordinate system of the structure) is calculated as

$$\langle \mathring{\mathbf{Q}}'^{(s)} \otimes \mathring{\mathbf{Q}}'^{(s)} \rangle = \hat{\mathbf{b}}^{(s)} \cdot \langle \mathring{\mathbf{Q}} \otimes \mathring{\mathbf{Q}} \rangle \cdot (\hat{\mathbf{b}}^{(s)})^T \tag{15}$$

where superscript "T" denotes transposition operation.

Using standard equations which express the laminate stiffnesses in terms of the reduced ply stiffness $\mathbf{Q}'^{(s)}$ and assuming that the reduced stiffnesses of individual plies are stochastically uncorrelated random functions, we obtain the following expressions of the covariance tensors of the laminate stiffnesses

$$\begin{aligned}
\langle \mathring{\mathbf{A}} \otimes \mathring{\mathbf{A}} \rangle &= \sum_{s=1}^{N} (\delta_s - \delta_{s-1}) \langle \mathring{\mathbf{Q}}'^{(s)} \otimes \mathring{\mathbf{Q}}'^{(s)} \rangle \\
\langle \mathring{\mathbf{B}} \otimes \mathring{\mathbf{B}} \rangle &= \frac{1}{4} \sum_{s=1}^{N} (\delta_s^2 - \delta_{s-1}^2)^2 \langle \mathring{\mathbf{Q}}'^{(s)} \otimes \mathring{\mathbf{Q}}'^{(s)} \rangle \\
\langle \mathring{\mathbf{D}} \otimes \mathring{\mathbf{D}} \rangle &= \frac{1}{9} \sum_{s=1}^{N} (\delta_s^3 - \delta_{s-1}^3)^2 \langle \mathring{\mathbf{Q}}'^{(s)} \otimes \mathring{\mathbf{Q}}'^{(s)} \rangle
\end{aligned} \tag{16}$$

and cross-covariance tensors of the laminate stiffnesses

$$\begin{aligned}
\langle \mathring{\mathbf{A}} \otimes \mathring{\mathbf{B}} \rangle &= \frac{1}{2} \sum_{s=1}^{N} (\delta_s - \delta_{s-1})(\delta_s^2 - \delta_{s-1}^2) \langle \mathring{\mathbf{Q}}'^{(s)} \otimes \mathring{\mathbf{Q}}'^{(s)} \rangle \\
\langle \mathring{\mathbf{A}} \otimes \mathring{\mathbf{D}} \rangle &= \frac{1}{3} \sum_{s=1}^{N} (\delta_s - \delta_{s-1})(\delta_s^3 - \delta_{s-1}^3) \langle \mathring{\mathbf{Q}}'^{(s)} \otimes \mathring{\mathbf{Q}}'^{(s)} \rangle \\
\langle \mathring{\mathbf{B}} \otimes \mathring{\mathbf{D}} \rangle &= \frac{1}{6} \sum_{s=1}^{N} (\delta_s^2 - \delta_{s-1}^2)(\delta_s^3 - \delta_{s-1}^3) \langle \mathring{\mathbf{Q}}'^{(s)} \otimes \mathring{\mathbf{Q}}'^{(s)} \rangle
\end{aligned} \tag{17}$$

where δ_s is the distance from the bottom laminate surface to the top surface of the sth layer. Equations (16) and (17) along with (12) and (15) provide all the necessary relations expressing the covariance tensors of the laminate in terms of standard deviations of the elastic constants of its layers.

4. THE IN-PLANE STRAIN/STRESS COVARIANCE ANALYSIS

The above theory is applicable for any lamination and any deformation mode (stretching, shearing, bending, torsion) of a thin-walled laminated structural element which can be accurately solved in the framework of classical deterministic theory of laminated plates and shells. Now we will further proceed with this analytical development considering symmetric laminations (in this case all elements of $\hat{\mathbf{B}}$ matrix are zero) and the in-plane loading conditions, when there are only membrane tractions acting on the structural element (all components of the $\mathbf{M}$ vector are zero). Accordingly, the constitutive equations (10) are uncoupled, and the strain vector is written as

$$\mathbf{e} = \hat{\mathbf{a}} \cdot \mathbf{N} \tag{18}$$

where $\hat{\mathbf{a}} = \hat{\mathbf{A}}^{-1}$. The strains $\varepsilon^{(s)}$ in the principal axes of symmetry of the sth layer and the strains $\mathbf{e}$ in the global axis of the structure are related through the equation

$$\varepsilon^{(s)} = \hat{\mathbf{g}}^{(s)} \cdot \mathbf{e} \tag{19}$$

where $\hat{\mathbf{g}}^{(s)}$ is the transformation matrix of the rotation through angle φ_s about the axis normal to the laminate mid-surface. The stresses expressed in the principal axes of symmetry of the sth layer are then calculated as

$$\sigma^{(s)} = \hat{\mathbf{Q}} \cdot \varepsilon^{(s)}. \tag{20}$$

Our next aim is to derive expressions for the covariance tensors of the strains $\varepsilon^{(s)}$ and stresses $\sigma^{(s)}$ in terms of the mean values and covariance tensors of the laminate stiffnesses and the load vector. The covariance tensor of the laminate compliances, $\langle \hat{\mathbf{a}} \otimes \hat{\mathbf{a}} \rangle$, is first needed for this purpose. To simplify the forthcoming calculations, we introduce the laminate compliance vector, $\mathbf{a}$, which contains only non-zero elements of the compliance tensor $\hat{\mathbf{a}}$. Then we shall calculate covariance tensor, $\langle \mathbf{a} \otimes \mathbf{a} \rangle$, for the vector $\mathbf{a}$. After that, all elements of the fourth order tensor $\langle \hat{\mathbf{a}} \otimes \hat{\mathbf{a}} \rangle$ can be derived by rearranging elements of the second order tensor $\langle \mathbf{a} \otimes \mathbf{a} \rangle$.

Each element of the compliance vector is a nonlinear function of the laminate membrane stiffnesses $\mathbf{A}$. To obtain the covariance functions of the laminate compliances, we again use the linearization procedure:

$$\mathbf{a} = \langle \mathbf{a} \rangle + \left. \frac{\partial \mathbf{a}}{\partial \mathbf{A}} \right|_{\mathbf{A} = \langle \mathbf{A} \rangle} \cdot (\mathbf{A} - \langle \mathbf{A} \rangle) + \cdots \approx \langle \mathbf{a} \rangle + (\mathbf{a} \nabla_A) \Big|_{\mathbf{A} = \langle \mathbf{A} \rangle} \cdot \mathring{\mathbf{A}} \tag{21}$$

where $\mathbf{a}\nabla_A$ is the second order tensor with its (i,j)th component equal to $\partial a_i / \partial A_j$. Making use of this expansion, one obtains the following covariance tensor of the compliance vector:

$$\langle \mathring{\mathbf{a}} \otimes \mathring{\mathbf{a}} \rangle = (\mathbf{a} \nabla_A)|_{\mathbf{A} = \langle \mathbf{A} \rangle} \cdot \langle \mathring{\mathbf{A}} \otimes \mathring{\mathbf{A}} \rangle \cdot (\nabla_A \mathbf{a})|_{\mathbf{A} = \langle \mathbf{A} \rangle} \tag{22}$$

where the (i,j)th component of the tensor $\nabla_A \mathbf{a}$ is equal to $\partial a_j / \partial A_i$.

Next we derive the strain covariance tensor. As it follows from (18), the centered strain vector can be written as

$$\mathring{\mathbf{e}} = \mathbf{e} - \langle \mathbf{e} \rangle = \hat{\mathbf{a}} \cdot \mathbf{N} - \langle \hat{\mathbf{a}} \rangle \cdot \langle \mathbf{N} \rangle. \tag{23}$$

By using (21), one obtains the following average tensor product of strain vectors:

$$\langle \mathring{\mathbf{e}} \otimes \mathring{\mathbf{e}} \rangle = \langle \mathring{\hat{\mathbf{a}}} \cdot \langle \mathbf{N} \rangle \otimes \mathring{\hat{\mathbf{a}}} \cdot \langle \mathbf{N} \rangle \rangle + \langle \hat{\mathbf{a}} \rangle \cdot \langle \mathring{\mathbf{N}} \otimes \langle \hat{\mathbf{a}} \rangle \cdot \mathring{\mathbf{N}} \rangle. \tag{24}$$

In derivation of (24), small terms of the fourth order such as $\mathring{\hat{\mathbf{a}}} \cdot \mathring{\mathbf{N}} \otimes \mathring{\hat{\mathbf{a}}} \cdot \mathring{\mathbf{N}}$, for example, have been neglected. Using the tensor identity $\hat{\mathbf{a}} \cdot \mathbf{N} = \mathbf{N} \cdot \hat{\mathbf{a}}^T$ and taking into account that $\hat{\mathbf{a}}$ is a symmetric tensor, (24) transforms into

$$\langle \mathring{\mathbf{e}} \otimes \mathring{\mathbf{e}} \rangle = \langle \mathbf{N} \rangle \cdot \langle \mathring{\hat{\mathbf{a}}} \otimes \mathring{\hat{\mathbf{a}}} \rangle \cdot \langle \mathbf{N} \rangle + \langle \hat{\mathbf{a}} \rangle \cdot \langle \mathring{\mathbf{N}} \otimes \mathring{\mathbf{N}} \rangle \cdot \langle \hat{\mathbf{a}} \rangle \tag{25}$$

where $\langle \mathring{\mathbf{N}} \otimes \mathring{\mathbf{N}} \rangle$ is the covariance tensor of the in-plane tractions, which is defined in terms of the random load characteristics. Using eqns (19) and (20), one obtains the following covariance matrices of the strains and stresses in the sth layer:

$$\langle \mathring{\varepsilon}^{(s)} \otimes \mathring{\varepsilon}^{(s)} \rangle = \hat{\mathbf{g}}^{(s)} \cdot \langle \mathring{\mathbf{e}} \otimes \mathring{\mathbf{e}} \rangle \cdot (\hat{\mathbf{g}}^{(s)})^T \tag{26}$$

$$\langle \mathring{\sigma}^{(s)} \otimes \mathring{\sigma}^{(s)} \rangle = \hat{\mathbf{Q}}^{(s)} \cdot \langle \mathring{\varepsilon}^{(s)} \otimes \mathring{\varepsilon}^{(s)} \rangle \cdot \hat{\mathbf{Q}}^{(s)}. \tag{27}$$

Equations (26) and (27) together with (25) and (22) provide all the necessary covariance relationships for the mesovolume reliability calculations.

5. CHARACTERIZATION OF THE RANDOM LOADS

Let the load vector $\mathbf{N}(t)$ be a Gaussian stochastic process represented in the form of a stochastically orthogonal spectral expansion

$$\mathbf{N}(t) = \langle \mathbf{N}(t) \rangle + \int_{-\infty}^{\infty} \mathbf{W}(\omega) e^{i\omega t} \, \mathrm{d}\omega \tag{28}$$

where the spectral vector $\mathbf{W}(\omega)$ satisfies the conditions of stochastic orthogonality

$$\langle \mathbf{W}^*(\omega) \otimes \mathbf{W}(\omega') \rangle = \hat{\mathbf{S}}_{\mathrm{N}}(\omega) \, \delta(\omega - \omega'). \tag{29}$$

Here, superscript "*" denotes complex conjugate, $\delta(\omega)$ is Dirac delta function, and $\hat{\mathbf{S}}_{\mathrm{N}}(\omega)$ is the tensor of spectral densities of the vector $\mathbf{N}(t)$. Tensor $\hat{\mathbf{S}}_{\mathrm{N}}(\omega)$ is related to the covariance tensor $\hat{\mathbf{K}}_{\mathrm{N}}(\tau)$ through the following relationships:

$$\hat{\mathbf{K}}_{\mathrm{N}}(\tau) = \langle \mathring{\mathbf{N}}(t+\tau) \otimes \mathring{\mathbf{N}}(t) \rangle = \int_{-\infty}^{+\infty} \hat{\mathbf{S}}_{\mathrm{N}}(\omega) e^{i\omega\tau} \, \mathrm{d}\omega$$

$$\hat{\mathbf{S}}_{\mathrm{N}}(\omega) = \frac{1}{2\pi} \int_{-\infty}^{\infty} \hat{\mathbf{K}}_{\mathrm{N}}(\tau) e^{-i\omega\tau} \, \mathrm{d}\tau \tag{30}$$

which constitutes the Wiener-Khintchine transform pairs. Although the covariance tensor $\hat{\mathbf{K}}_{\mathrm{N}}(\tau)$ is invariant regarding the time reference point, the random process $\mathbf{N}(t)$ specified by the expansion (28) is, generally, not a stationary one since its mathematical expectation $\langle \mathbf{N}(t) \rangle$ may be an arbitrary function of time. Evidently, centered load vector $\mathring{\mathbf{N}}(t) = \mathbf{N}(t) - \langle \mathbf{N}(t) \rangle$ is a stationary stochastic process.

According to eqn (8), in order to calculate the rate of crossings of the prescribed positive or negative ultimate level, one has to obtain the covariance matrix of the derivatives of the performance vector. By performing double differentiation in eqn (25) with respect to time variable, and taking into account relations (28) and (29), one obtains the following covariance tensor of the strain derivatives:

$$\left\langle \frac{\mathrm{d}\mathring{\mathbf{e}}}{\mathrm{d}t} \otimes \frac{\mathrm{d}\mathring{\mathbf{e}}}{\mathrm{d}t} \right\rangle = \langle \dot{\mathbf{N}}(t) \rangle \cdot \langle \mathring{\mathbf{a}} \otimes \mathring{\mathbf{a}} \rangle \cdot \langle \dot{\mathbf{N}}(t) \rangle - \langle \hat{\mathbf{a}} \rangle \cdot \ddot{\hat{\mathbf{K}}}_{\mathrm{N}}(0) \cdot \langle \hat{\mathbf{a}} \rangle \tag{31}$$

where $\dot{\mathbf{N}}(t)$ and $\ddot{\hat{\mathbf{K}}}_{\mathrm{N}}(t)$ are first and second time derivatives of functions $\mathbf{N}(t)$ and $\hat{\mathbf{K}}_{\mathrm{N}}(t)$, respectively. By making use of the (31), (19) and (20), the covariance tensors of the strain and stress derivatives related to the material axes can be easily evaluated.

7. NUMERICAL EXAMPLES

7.1. *Laminated cylindrical shells under internal pressure*

In the framework of the general method developed, we further solve several specific problems to illustrate the effects of scatters in elastic and strength characteristics of the material and random loading histories on the reliability function. First example considers laminated circular cylindrical shell made of identical Kevlar fiber reinforced polymeric layers. Geometrical parameters of the shell are: $h = 5 \cdot 10^{-3} m$, $R_0/h = 200$, $L/R_0 = 2$, where h is the thickness, L is the length, and R_0 is the radius of the mid-surface. The data of

Table 1. Elastic and strength characteristics of the unidirectional Kevlar/epoxy composite

Material characteristic†	Mean value	Standard deviation, %
	Elastic constants	
E_{11}, GPa	74.9	2.97
E_{22}, GPa	4.65	3.44
G_{12}, GPa	1.8777	1.76
ν_{12}	0.35	8.86
	Ultimate strains	
ε_{11}^{-}	$-0.478 \cdot 10^{-2}$	5.2
ε_{11}^{+}	$1.71 \cdot 10^{-2}$	11.7
ε_{22}^{-}	$-1.41 \cdot 10^{-2}$	7.8
ε_{22}^{+}	$0.283 \cdot 10^{-2}$	5.6
$\varepsilon_{12}^{\pm}$	$\pm 2.56 \cdot 10^{-2}$	30.8

† *Note*: subscript "1" corresponds to the fiber direction, "2" to the transverse direction.

Table 1, taken from Clements and Chiao (1977), will be used as input data in our calculations of the random stiffnesses, compliances and strength characteristics of the monolayer.

Consider a circular cylindrical shell under the effect of stochastic axisymmetric internal pressure. In this case, each layer in the shell can be treated as the mesovolume, and its performance is characterized by the random process depending on time but not on space coordinates. The applied random internal pressure $p(t)$ is defined by its mean $\langle p(t) \rangle$ and random fluctuations around this mean. The fluctuations are defined by the following covariance function:

$$K_p(\tau) = \sigma_p^2 \exp\left(-\frac{\tau^2}{\tau_0^2}\right) \tag{32}$$

which corresponds to the Gaussian distribution of the spectral density. The parameters σ_p and τ_0 correspond to the standard deviation and correlation time of the random fluctuations.

According to the membrane shell theory, the traction vector for cylindrical shell having end closures and loaded with internal pressure $p(t)$ is defined as $\mathbf{N}(t) = \{p(t)R_0/2, p(t)R_0, 0\}$. Thus, the covariance tensor of the traction vector and the covariance tensor of its derivative are of the form

$$\langle \mathring{\mathbf{N}} \otimes \mathring{\mathbf{N}} \rangle = R_0^2 \sigma_p^2 \hat{\Omega}, \langle \mathring{\dot{\mathbf{N}}} \otimes \mathring{\dot{\mathbf{N}}} \rangle = \frac{R_0^2 \sigma_p^2}{\tau_0^2} \hat{\Omega} \tag{33}$$

where

$$\hat{\Omega} = \begin{bmatrix} 1/4 & 1/2 & 0 \\ 1/2 & 1 & 0 \\ 0 & 0 & 0 \end{bmatrix}. \tag{34}$$

The performance vector is then specified in three-dimensional strain space in such a way as its components are the strain tensor components referred to the principal axes of the sth layer:

$$\mathbf{q}^{(s)}(t) = \{\varepsilon_{11}^{(s)}(t), \varepsilon_{22}^{(s)}(t), \varepsilon_{12}^{(s)}(t)\}. \tag{35}$$

The rate of "decay" of the shell reliability during some specific random load history is controlled by the following stochastic factors:

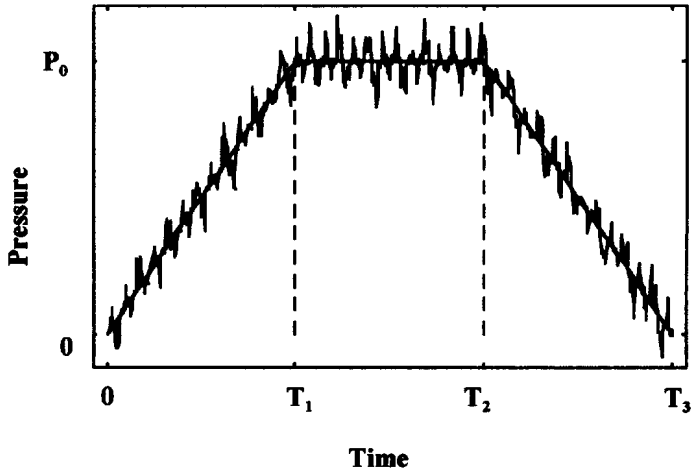

Fig. 1. Illustration of the random loading history of a cylindrical shell.

(i) random time-dependence of the applied internal pressure,
(ii) scatter in elastic constants of the monolayer, and
(iii) scatter in ultimate strains of the monolayer.

We will further examine the effect of all these factors. All of the shells under consideration were composed of four symmetrically placed identical Kevlar/epoxy layers, but with varying ply lay-ups. Thus, the total shell thickness is the same in all of the examples. Input parameters of the mean internal pressure (see Fig. 1) are: $T_1 = 10$s, $T_2 = 20$s, $T_3 = 30$s, $p_0 = 0.7p_\varphi^*$, where p_φ^* is the value of the "critical" deterministic internal pressure. This critical value, specific for each particular lamination, is defined from the solution of the corresponding deterministic first-ply failure problem. The first-ply failure is calculated for the laminated shells under consideration using mean values of the material properties listed in Table 1.

Numerical results shown in Figs 2 and 3 correspond to $[0°, 90°]_s$ laminated shell. The calculated value of p_φ^* is 0.578 MPa. These results illustrate that the reliability decreases with the increase of the standard deviation of the internal pressure and the decrease of the correlation time. The dependence of the reliability function on the correlation time τ_0 can be easily explained. The correlation time characterizes attenuation of the correlation between the stochastic process parameters at different time instants. When the correlation time is decreased, the frequency of fluctuations of the stochastic process is increased (with their average amplitude being the same). Consequently, the number of "attempts" to cross the prescribed ultimate level in some time interval is increased. Obviously, under the condition that all other input parameters are fixed, but the number of attempts is increased, the result is the lower value of the reliability. In the other words, the higher is the frequency of random fluctuations of the random load history, the more significantly these fluctuations affect the reliability function.

The effect of the scatter in elastic constants and ultimate strains on the reliability function is shown in Fig. 4. The results correspond to ply lay-up $[0°, 90°]_s$. The correlation time τ_0 is 0.01 s in all cases. Standard deviation of the applied pressure is 10% of the maximum level, and the maximum level is 70% of the critical deterministic internal pressure value for this specific shell. As seen from Fig. 4, the fluctuations of the applied load and the scatter in elastic constants substantially decrease the reliability. However, the effect of the scatter in ultimate strains is even more pronounced. If both the scatters are taken into account simultaneously (curve 3), the most rapid drop of the reliability is obtained. Certainly, the quantitative effect of the examined random factors on the reliability function depends on the specific ply lay-up. Many additional calculations performed allowed us to conclude that the most severe effect was always due to the scatter in ultimate strains, not due to the scatter in elastic properties. The conclusion is valid for the loading case under consideration and the composite material treated here regardless of the specific ply lay-ups.

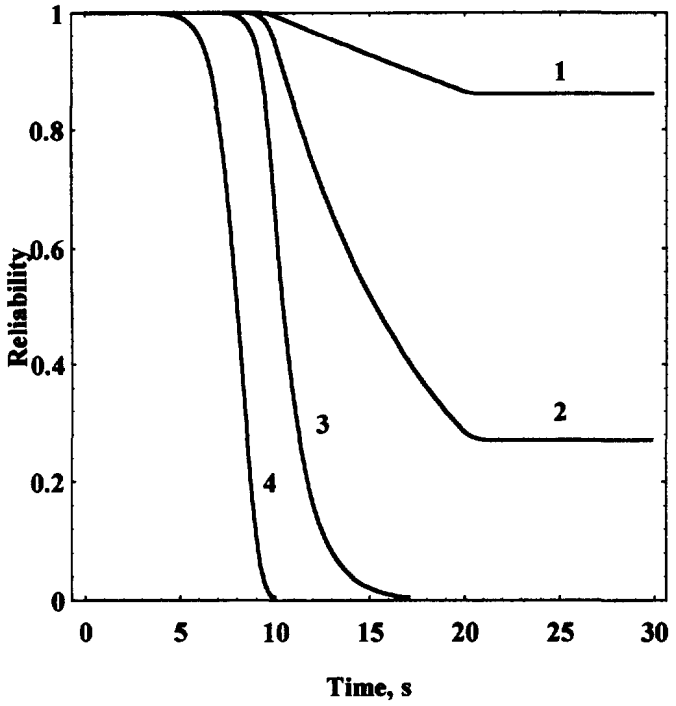

Fig. 2. Reliability functions at different values of the random load standard deviations (in % of the maximum load level $p_0 = 0.7p_\varphi^*$) : curve 1–1%, curve 2–5%, curve 3–10%, curve 4–20%. Correlation time $\tau_0 = 0.01$ s in all cases.

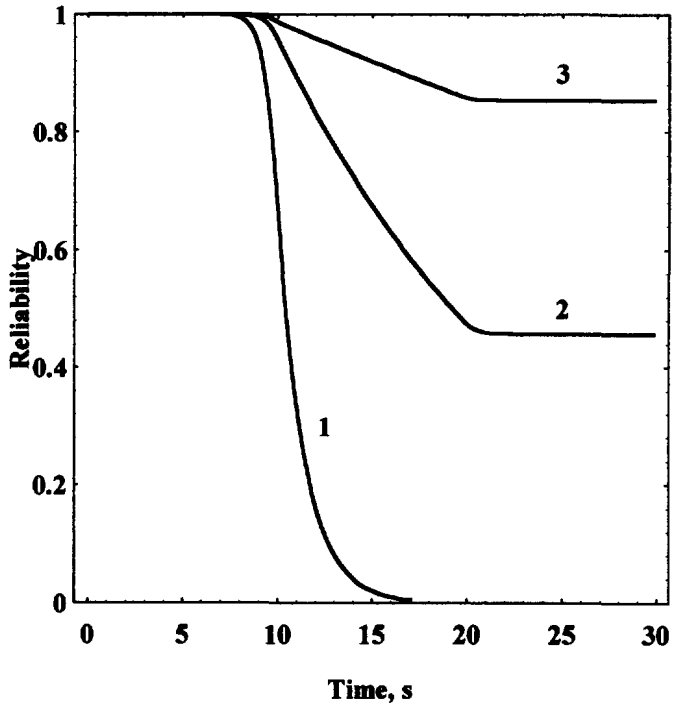

Fig. 3. Reliability functions at different values of the random load correlation time τ_0 : 0.01 s (curve 1), 0.1 s (curve 2), 0.5 s (curve 3). Standard deviation of the load value is 10% of the maximum load level $p_0 = 0.7p_\varphi^*$.

This result is, probably, a consequence of the higher variance of the ultimate strains than that of the elastic characteristics for the considered composite material.

Effect of the ply lay-up on the reliability function is illustrated in Fig. 5. The following ply lay-ups have been considered : $[0, 90°]_s$ (case I), $[30°, -30°]_s$ (case II), $[40°, -40°]_s$ (case

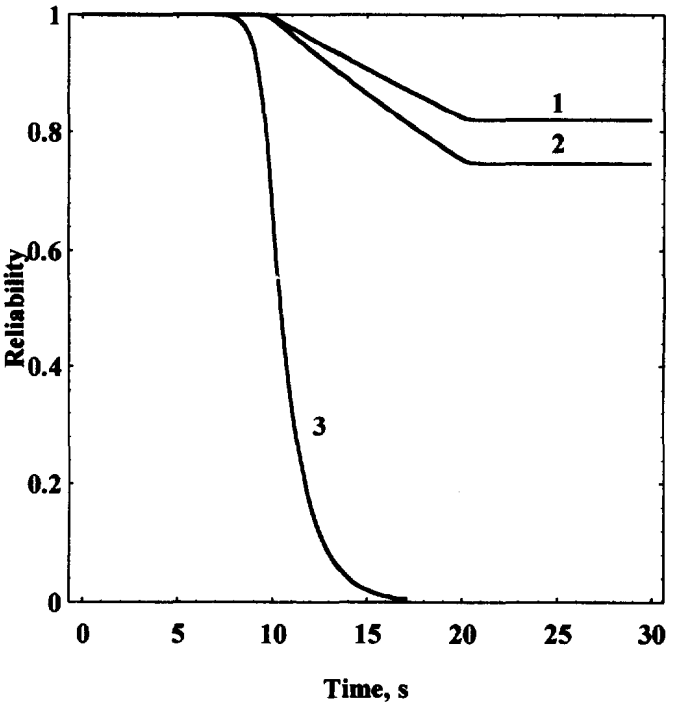

Fig. 4. Reliability functions calculated with account of: random load history (curve 1), random load history and scatter in elastic characteristics (curve 2), random load history and scatter in elastic and strength characteristics (curve 3). Standard deviation of the load value is 10% of the maximum load level $p_0 = 0.7p_\varphi^*$. Correlation time $\tau_0 = 0.01$ s in all cases.

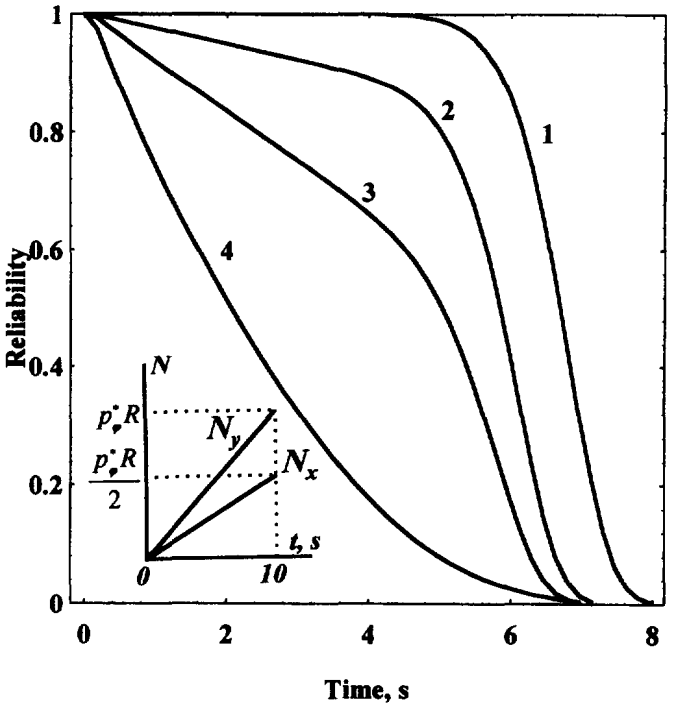

Fig. 5. Reliability function for the shells with ply lay-ups $[0°, 90°]_s$ (curve 1), $[30°, -30°]_s$ (curve 2), $[40°, -40°]_s$ (curve 3), and $[45°, -45°]_s$ (curve 4). Standard deviation of the load value is 10% of p_φ^*. Correlation time $\tau_0 = 0.01$ s in all cases.

III), and $[45°, -45°]_s$ (case IV). Each of the curves has been calculated under its own random load history, therefore their mutual comparison does not say much. Specifically, a linearly increasing loading path with the loading rate $0.1p_\varphi^*$ has been used for all of the

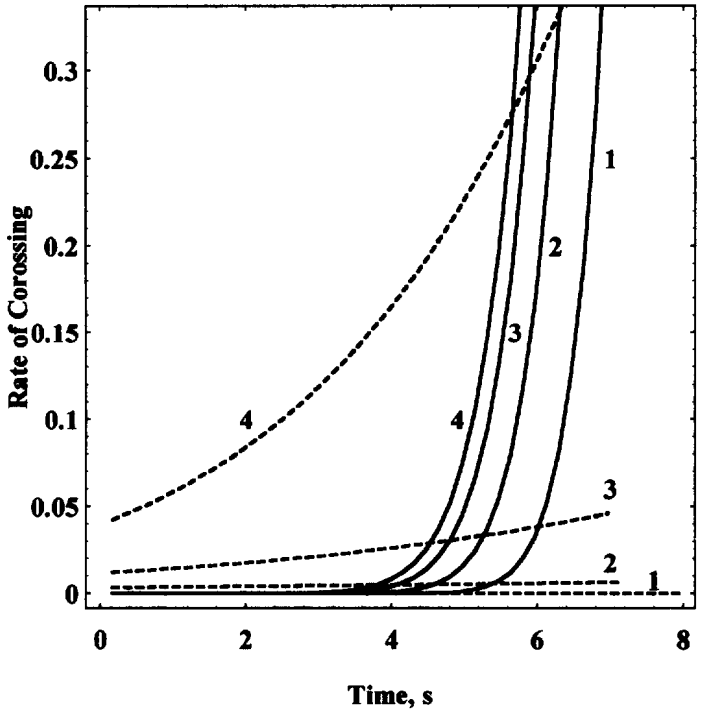

Fig. 6. Dependencies of the expected rates of crossings of the ultimate level on time. Solid lines correspond to $\nu[\varepsilon_{22}(t)\,;\varepsilon_{22}^{+}]$, dashed lines to $\nu[\varepsilon_{12}(t)\,;\varepsilon_{12}^{\pm}]$. Ply lay-ups: $[0, 90°]_s$ (curve 1), $[30°, -30°]_s$ (curve 2), $[40°, -40°]_s$ (curve 3), and $[45°, -45°]_s$ (curve 4).

variants, but the value of p_φ^* (corresponding to the deterministic first-ply failure) is distinct for all the lamination cases. The values of p_φ^* are: 0.578 MPa for the case I, 0.113 MPa for II, 0.297 MPa for III, and 0.787 MPa for IV. Note that loading paths were specified in such a way that in the deterministic problem, first-ply failure occurs at the same time instant, namely $t = 10$ s, for all four cases. Standard deviations of the applied internal pressure, σ_p, were taken 10% of p_φ^* for all of the cases (here again, p_φ^* has been calculated for each specific lamination case). Solution of the deterministic problem showed that in the case I first-ply failure occurred simultaneously in 0° layers and was caused by the transverse tensile normal strain ε_{22}. In the cases II–IV, first-ply failure occurred simultaneously in all $\pm\varphi$ layers, and also due to the strain component ε_{22}. It is interesting to note that, according to Fig. 5, the reliability function has a very different shape depending on the ply lay-up. Some of the curves are rather shallow, others show a very sharp drop of reliability in a rather narrow time interval.

Some explanation of the calculated variations of the reliability function can be obtained from the results presented in Fig. 6. Here, variations of the rates of crossings, $\nu[\varepsilon_{22}(t)\,;\varepsilon_{22}^{+}]$ and $\nu[\varepsilon_{12}(t)\,;\varepsilon_{12}^{\pm}]$, of the ultimate levels on time are shown. The rest of the expected rates of crossings have much lower values. Solid lines indicate the rates of the up-crossing of the ultimate level ε_{22}^{+} and dashed lines indicate the rates of crossings of the ultimate level $\varepsilon_{12}^{\pm}$. It is seen that for the case I the drop of reliability is caused by the tensile transverse strain only. For the cases II–IV, there is a time instant, t_*, at which the rates of up-crossings of the ultimate level ε_{22}^{+} and the rates of crossings of the ultimate level $\varepsilon_{12}^{\pm}$ are equal. This means that the drop in reliability at this time instant is caused, to an equal extent, by ε_{12} and ε_{22}. At $t < t_*$, the first-ply failure due to ε_{12} is most probable, whereas at $t > t_*$ the first-ply failure of the same layers is most probable due to ε_{22}. A high probability of different first-ply failure modes is a consequence of a large scatter of the ultimate shear strains (the adopted standard deviation is higher than 30%). Even if the mean value of the shear strain is much lower than its ultimate value, there is a non-zero rate of crossing of the ultimate levels $\varepsilon_{12}^{\pm}$ as indicated by dashed curve 2 in Fig. 6. With increasing shear strains, the rate of

crossings of the ultimate level $\varepsilon_{12}^{\pm}$ increases, and more pronounced contribution of the shear failure mode to the drop of reliability is predicted.

7.2. *Laminated rectangular plates under biaxial loading*

Second example considers laminated plates under proportional biaxial in-plane random loading. The plate of thickness $h = 5 \cdot 10^{-3}$ m with the layer properties described in Table 1 is solved. The applied tractions $N_x(t)$ and $N_y(t)$ form a random vector $\mathbf{N}(t) = \{N_x(t), N_y(t), 0\}$ with its mean non-zero components defined as

$$\langle N_x(t) \rangle = N_x^* \cdot t \cdot \cos\alpha, \quad \langle N_y(t) \rangle = N_y^* \cdot t \cdot \sin\alpha \tag{36}$$

where N_x^* and N_y^* are some constants specified for each particular ply lay-up. Equation (36) covers all possible paths of proportional in-plane biaxial loadings as α varies from 0 to 2π. The covariance tensor of random fluctuations of the load vector and the covariance tensor of its derivative are of the form

$$\langle \mathring{\mathbf{N}} \otimes \mathring{\mathbf{N}} \rangle = \begin{bmatrix} \sigma_{N_x}^2 & 0 & 0 \\ 0 & \sigma_{N_y}^2 & 0 \\ 0 & 0 & 0 \end{bmatrix}, \quad \langle \dot{\mathring{\mathbf{N}}} \otimes \dot{\mathring{\mathbf{N}}} \rangle = \frac{1}{\tau_0^2} \langle \mathring{\mathbf{N}} \otimes \mathring{\mathbf{N}} \rangle \tag{37}$$

where σ_{N_x} and σ_{N_y} are standard deviations of the tractions $N_x(t)$ and $N_y(t)$, respectively. Diagonal form of the matrix of the load covariance tensor in (37) suggests that random fluctuations of the load components are not correlated.

Figures 7 and 8 illustrate reliability surfaces for laminated plates with ply lay-ups $[60°, -60°]_s$ and $[30°, -30°, 90°]_s$, respectively. Standard deviations of the applied tractions are: $\sigma_{N_x} = 0.1 N_x^*$ and $\sigma_{N_y} = 0.1 N_y^*$. Here, N_x^* is the value of the traction defined from the solution of the corresponding deterministic first-ply failure problem, when only uniaxial tensile load $\mathbf{N} = \{N_x, 0, 0\}$ is applied in the x direction. Similarly, N_y^* is the value of the traction defined from the solution of the corresponding deterministic first-ply failure problem when only a uniaxial tensile load $\mathbf{N} = \{0, N_y, 0\}$ is applied in the y direction. The ultimate surfaces related to the corresponding deterministic first-ply failure problems are also presented in Figs 7 and 8 using dashed lines. The values $N_x^* = 0.0965$ MPa·m, $N_y^* = 1.674$ MPa·m were obtained for the laminate $[60°, -60°]_s$ and $N_x^* = 0.396$MPa·m, $N_y^* = 0.594$ MPa·m for the laminate $[30°, -30°, 90°]_s$. Solid lines in Figs 7 and 8 show a series of concentric surfaces, each corresponding to a different reliability index, in the space of mean tractions.

Ultimate surface of the laminate $[60°, -60°]_s$ (Fig. 7a) is highly directional, which indicates a sensitivity of the plate to small deviations from the applied loads. Indeed, small fluctuations of the load vector ($\approx 10\%$) result in a violent collapse of the reliability surface even for the low values of the reliability indices (Fig. 7b). In addition, the shape of the reliability surfaces completely differs from that of the deterministic ultimate surface. This indicates that additional failure modes (which are not predicted in the deterministic failure analysis) appear in the stochastic failure process. Further, it is seen in Fig. 8 that the reliability surfaces of the laminate $[30°, -30°, 90°]_s$ are far less directional and less collapsed, at least for the moderate values of the reliability indices. Consequently, this type of lamination is less sensitive to the changes in the elastic and strength properties of the material as well as to the loading conditions.

The above examples illustrate that the developed approach can be efficiently used in the optimization problems with the constraints formulated in terms of the reliability index.

8. COMPARISON WITH MONTE CARLO SIMULATION RESULTS

Monte Carlo simulations have been carried out in this work to verify the results obtained with the developed novel analytical approach. To perform the Monte Carlo

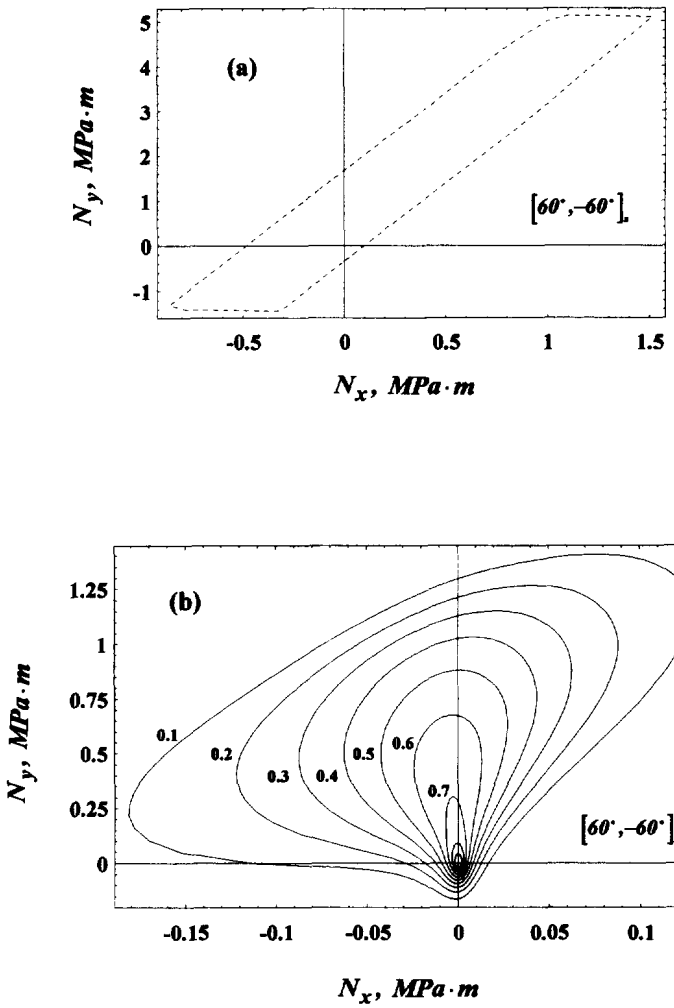

Fig. 7. The deterministic ultimate surface (a) and the reliability surfaces (b) for the laminate $[60°, -60°]_s$ under biaxial proportional loading. Numbers indicate the values of reliability index.

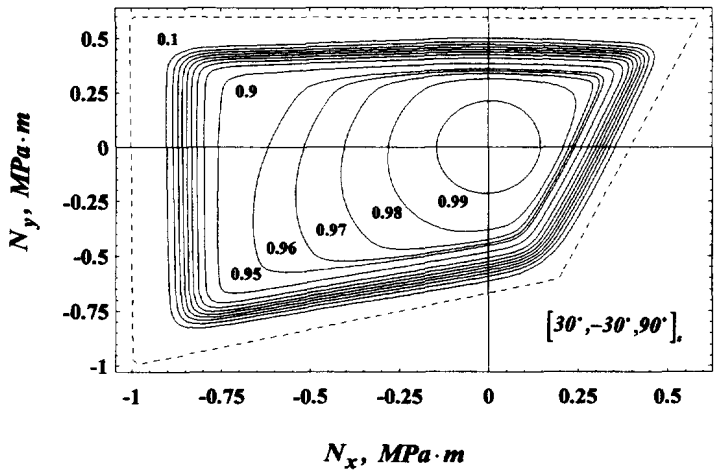

Fig. 8. The deterministic ultimate surface (dashed line) and the reliability surfaces (solid lines) for the laminate $[30°, -30°, 90°]_s$ under biaxial proportional loading. Numbers indicate the values of reliability index.

simulation, the random input data has to be generated first. The random elastic and strength characteristics of the composite material have been generated using standard procedure for the generation of random numbers with Gauss distribution function (Press *et al.*, 1992). A random process is modeled using the discrete approximation of the spectral expansion (28):

$$\mathbf{N}(t) \approx \langle \mathbf{N}(t) \rangle + \sum_{k=1}^{K} (\mathbf{U}_k \cos \omega_k t + \mathbf{V}_k \sin \omega_k t) \tag{38}$$

where $\mathbf{U}_k$ and $\mathbf{V}_k$ are independent Gaussian vectors having the following properties

$$\langle \mathbf{U}_k \rangle = \langle \mathbf{V}_k \rangle = 0, \quad \langle \mathbf{U}_k \otimes \mathbf{V}_k \rangle = 0, \quad \langle \mathbf{U}_k \otimes \mathbf{U}_l \rangle = \langle \mathbf{V}_k \otimes \mathbf{V}_l \rangle = 2\hat{\mathbf{S}}_N(\omega_k)\, \Delta\omega \delta_{kl}. \tag{39}$$

Here, $\omega_k = k\Delta\omega$, $\Delta\omega = \omega_c/K$, ω_c is an upper cut-off frequency beyond which the spectral density may be assumed to be zero, and δ_{kl} is the Croneker delta. Approximation (38) is asymptotically a Gaussian stochastic process as $K \to \infty$ (Shinozuka and Deodatis, 1991).

Since the following consideration deals with the not-correlated components of the random loading, it is sufficient to examine the details of the scalar random process modeling. The spectral density of the scalar stochastic process $N(t)$ with exponential covariance function of the type (32) is expressed according to the second relation of (30), as follows:

$$S_N(\omega) = \frac{\sigma_N^2 \tau_0}{2\sqrt{\pi}} \exp\left(-\frac{\omega^2 \tau_0^2}{4}\right). \tag{40}$$

Note that the random process defined by (40) is differentiable, since

$$\int_{-\infty}^{+\infty} \omega^2 S_N(\omega)\, \mathrm{d}\omega < \infty. \tag{41}$$

The plot of the spectral density (40) of the random load fluctuations is shown in Fig. 9a. The cut-off frequency is specified here as

$$\omega_c = 2\pi/\tau_0. \tag{42}$$

It is seen from Fig. 9a that at $\omega \geqslant \omega_c$, the spectral density is very close to zero. Spectral density defines completely the nature of the internal pressure random fluctuation. The realizations of these fluctuations modeled by the discrete approximation (38) for several values of K are presented in Fig. 9b. One can observe that the pseudo-period of random fluctuations increases with the increase of the number of approximating terms in (38). Indeed, it can be shown that the simulated stochastic process given by eqn (38) has the period

$$T_K = \frac{2\pi}{\Delta\omega} = \frac{2\pi K}{\omega_c}. \tag{43}$$

Referring to eqn (42) for the cut-off frequency, one obtains $T_K/\tau_0 = K$.

Monte Carlo simulations have been performed for the laminate $[30°, -30°, 90°]_s$ considered in the second example of Section 8. The results of Monte Carlo simulation are illustrated for two specific loading paths: $\alpha = \pi/2$ and $\alpha = \pi/6$ which, according to eqn (36), correspond to uniaxial and biaxial in-plane loading cases, respectively. Twenty terms ($K = 20$) in approximation (38) have been used to model the random processes. For each loading path, 100 Monte Carlo runs have been performed. Results of the Monte Carlo runs were grouped in bins of size $\Delta t = 0.08$ s to obtain the histogram of the first-ply failure probability density; those are presented in Fig. 10 by open symbols. The data were then smoothed by applying a Stineman function, and the final results are shown in Fig. 10 by

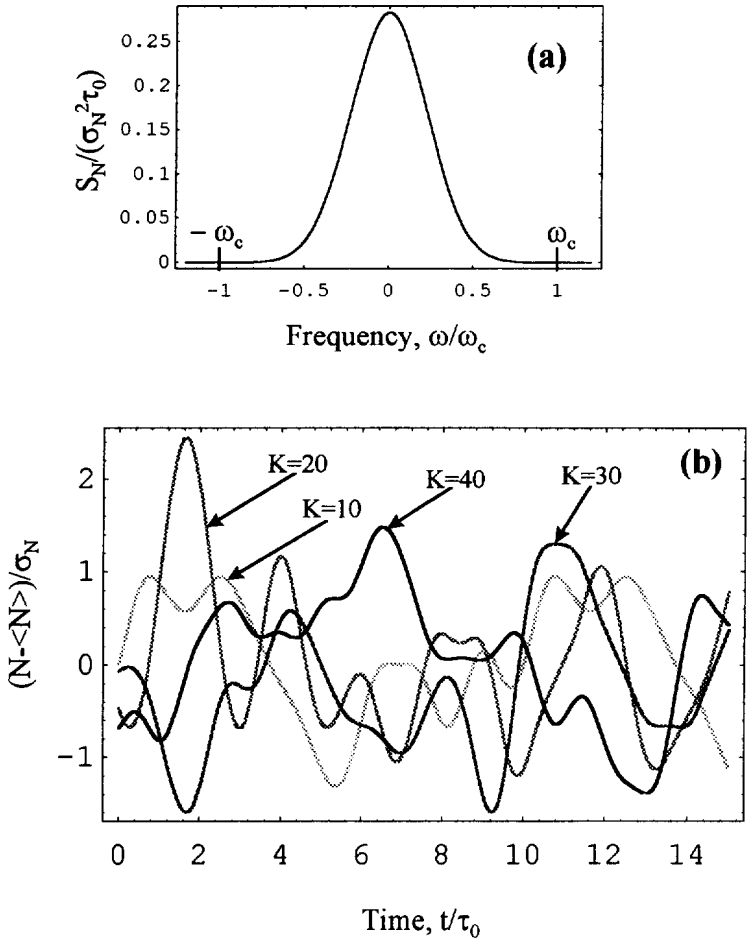

Fig. 9. Spectral density (a) and realization (b) of the load fluctuations. Correlation time $\tau_0 = 0.01$ s.

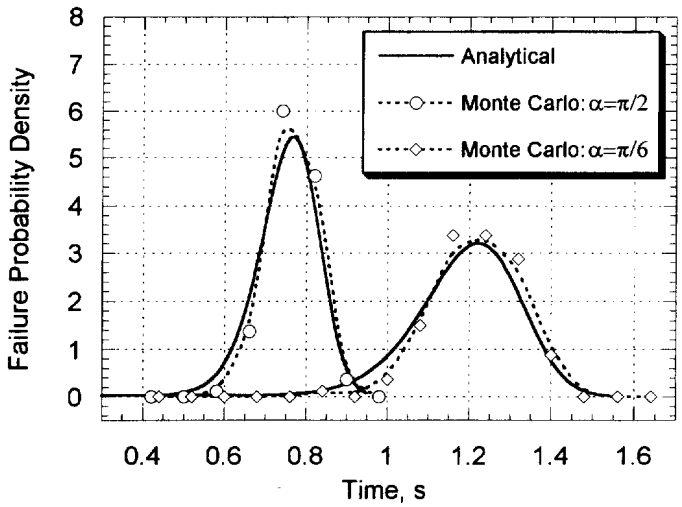

Fig. 10. Comparison of the results obtained with Monte Carlo simulation (open symbols and dotted lines) and with the developed analytical method (solid lines) for $[30°, -30°, 90°]_s$ laminate under uniaxial loading ($\alpha = \pi/2$) and biaxial in-plane proportional loading ($\alpha = \pi/6$).

dotted lines. Numerical results obtained for the same problem from the developed analytical method are shown by solid lines. It is seen that correspondence between both groups of results is very good. This verifies applicability and accuracy of the developed analytical

approach. In particular, the assumption that crossings of the ultimate level are rare events is validated, and applicability of the probabilistic linearization procedure used for the evaluation of the standard deviation of the performance vector is justified.

Finally, it has to be pointed out that in order to obtain the curves presented in Fig. 10, about 100 times more CPU time is required when using Monte Carlo simulation, compared to the developed analytical method. It also has to be emphasized that when considering higher reliability indices, the number of required Monte Carlo runs is sharply increasing. This causes a proportional increase in CPU time consumption. On the contrary, when performing reliability simulation using the developed analytical approach, CPU time is independent of the reliability index.

9. CONCLUSIONS

- The developed novel mathematical approach and computational algorithm utilize advanced theory of stochastic processes, namely, the analysis of rare passages of the vector stochastic process beyond the stochastic limiting surface.
- The approach allows one to calculate the reliability function of laminated composite plates and shells with account for (i) random complex loading history, (ii) scatter in the elastic properties of the lamina, (iii) scatter in the ultimate strains or stresses of the lamina. Any loading case which can be solved in terms of the in-plane normal and shear tractions can be analyzed using this approach.
- Illustrative examples show that failure mechanisms in the probabilistic initial failure problems are substantially more complex than those in the corresponding deterministic problems. Any of the above factors (i), (ii) or (iii) may have a detrimental effect on the reliability, although in the studied case the most severe effect was due to the scatter in ultimate strains.
- Monte Carlo simulations presented in the work for a comparison verify applicability and accuracy of the developed analytical approach. Numerical examples studied in this work show that the proposed analytical approach allows one to reduce computational expenses at least 100 times as compared to Monte Carlo methodology.
- Probabilistic analysis of laminated composite plates and shells provides substantially more information when considering gradual stochastic failure processes. In this case, even for a rather small number of layers, there is a great variety of probabilistic "branches" of the stochastic failure process. Accordingly, an ultimate failure prediction would necessarily be the result of many "competitive" probabilistic paths of failure. This type of analysis will be addressed in our future work.

Acknowledgements—This work was financially supported by Office of Naval Research through Grant No. N00014-95-1-0642, Dr Yapa D. S. Rajapakse is the grant monitor.

REFERENCES

Bogdanovich, A. E. and Yushanov, S. P. (1981) Analysis of the buckling of cylindrical shells with random field of initial imperfections under axial dynamic compression. *Mechanics of Composite Materials* **17**(5), 821–831 (in Russian).

Bogdanovich, A. E. and Yushanov, S. P. (1983) Computing the reliability of anisotropic shells from the probability of infrequent excursions of a random vector field beyond the limiting surface. *Mechanics of Composite Materials* **19**(1), 80–89 (in Russian).

Bogdanovich, A. E. and Yushanov, S. P. (1987) A reliability analysis of laminated composites and cylindrical shells. In *Proceedings of the Sixth International Conference on Composite Materials and Second European Conference on Composite Materials*, vol. 5. Elsevier Applied Science, London and New York, pp. 5.525–5.535.

Bogdanovich, A. E. and Yushanov, S. P. (1994) Probabilistic modeling of dynamic buckling and failure of imperfect laminated composite shells. In *Proceedings of the International Mechanical Engineering Congress and Exposition*, Chicago, 1994, AD-Vol. 43. *Durability and Damage Tolerance*. ASME publications, New York, pp. 19–35.

Bolotin, V. V. (1976) Statistical theory of defect buildup in composite materials and the scale-factor effect in reliability. *Polymer Mechanics* **12**(2), 247–255 (in Russian).

Bolotin, V. V. (1981) A unified model of the breakdown of composite materials in the case of long-acting loads. *Mechanics of Composite Materials* **17**(3), 405–420 (in Russian).

Bolotin, V. V. (1982) *Methods of the Theory of Probability and Theory of Reliability in the Structural Analysis*. Stroiizdat, Moscow.

Cassenti, B. N. (1984) Probabilistic static failure of composite materials. *AIAA Journal* **22,** 103–110.
Cederbaum, G., Elishakoff, I. and Librescu, L. (1990) Reliability of laminated plates via the first-order second-moment method. *Composite Structures* **15,** 161–167.
Corvi, A. and Vangi, D. (1992) A structural reliability model for composite materials. *Quality and Reliability Engineering International* **8,** 523–530.
Clements, L. L. and Chiao, T. T. (1977) Engineering design data for an organic fibre/epoxy composite. *Composites* **8**(2), 87–92.
Dzenis, Yu. A., Joshi, S. P. and Bogdanovich, A. E. (1992) Damage evolution modeling in orthotropic laminated composites. In *Proceedings of the AIAA/ASME/ASCE/AHS/ASC 33rd Structures, Structural Dynamics, and Materials Conference*, 1992, Pt. 5. AIAA, Washington, DC, pp. 2887–2897.
Dzenis, Yu. A., Joshi, S. P. and Bogdanovich, A. E. (1993) Behavior of laminated composites under monotonically increasing random load. *AIAA Journal* **31**(12), 2329–2334.
Dzenis, Yu. A., Joshi, S. P. and Bogdanovich, A. E. (1994) Damage evolution modeling in orthotropic laminated composites. *AIAA Journal* **32**(2), 357–364.
Engelstad, S. P. and Reddy, J. N. (1992) Probabilistic nonlinear finite element analysis of composite structures. *AIAA Journal* **31**(2), 362–369.
Jones, R. M. (1975) *Mechanics of Composite Materials*. Hemisphere Publishing Corporation, New York.
Kam, T. Y., Lin, S. C. and Hsiao, K. M. (1993) Reliability analysis of nonlinear laminated composite plate structures. *Composite Structures* **25,** 503–510.
Nakagiri, S., Takabatake, H. and Tani, S. (1987) Uncertain eigenvalue analysis of composite laminated plates by the stochastic finite element method. *Journal of Engineering for Industry* **109**(1), 9–12.
Press, W. H., Tenkolsky, S. A., Vettering, W. T. and Flannery, B. P. (1992) *Numerical Recipes in FORTRAN: The Art of Scientific Computing*, second edition. Cambridge University Press, New York.
Protasov, V. D. and Ermolenko, A. F. (1983) Problems of the strength of shell designs fashioned from wound composites. *Mechanics of Composite Materials* **19**(6), 1034–1043 (in Russian).
Protasov, V. D., Ermolenko, A. F., Filipenko, A. A. and Dimitrienko, I. P. (1978) Strength and reliability of cylindrical shells prepared by the method of continuous filament winding. *Polymer Mechanics* **14**(3), 443–451 (in Russian).
Protasov, V. D., Ermolenko, A. F., Filipenko, A. A. and Dimitrienko, I. P. (1980) Investigation of the supporting capacity of laminated cylindrical shells with the help of a computer simulation of the fracture process. *Mechanics of Composite Materials* **16**(2), 254–261 (in Russian).
Shinozuka, M. and Deodatis, G. (1991) Simulation of stochastic processes by spectral representation. *Applied Mechanics Review* **44**(4), 191–204.
Sveshnikov, A. A. (1968) *Applied Methods of Random Functions*. Pergamon Press, New York.
Tani, S., Nakagiri, S. and Higashino, T. (1988) Assessment of the reliability indices of CFRP laminated plate. In *Computational Probabilistic Methods*, eds W. K. Lui *et al.* ASME-AMD-93, Berkeley, CA, pp. 27–36.
Thanedar, P. B. and Chamis, C. C. (1995) Reliability considerations in composite laminate tailoring. *Computers & Structures* **54**(1), 131–139.
Thomas, D. J. and Wetherhold, R. C. (1991) Reliability analysis of continuous fiber composite laminates. *Composites Structures* **17,** 277–293.
Yushanov, S. P. (1985a) Calculation of the reliability of composite laminated shells with random elastic and strength characteristics. *Mechanics of Composite Materials* **21**(1), 87–96 (in Russian).
Yushanov, S. P. (1985b) A probability model of layer-by-layer failure of a composite and calculation of the reliability of laminated cylindrical shells. *Mechanics of Composite Materials* **21**(4), 642–652 (in Russian).
Yushanov, S. P. and Bogdanovich, A. E. (1986) Method of computing the reliability of imperfect laminar cylindrical shells with allowance for scatter in the strength characteristics of the composite material. *Mechanics of Composite Materials* **22**(6), 1043–1048 (in Russian).